

# [EN-042] Development of GBAS Ionosphere Anomaly Monitor Standards to Support Category III Operations

<sup>+</sup>M. Harris\*, T. Murphy\*, S. Saito\*\*

\*Boeing Commercial Airplanes  
Airplane Systems/Air Traffic Management  
Seattle, WA, USA

\*\*Electronic Navigation Research Institute (ENRI)  
Tokyo, Japan

**Abstract:** This paper summarizes work done by Boeing and Electronic Navigation Research Institute (ENRI) to validate proposed Ground Based Augmentation System (GBAS) requirements intended to mitigate the effects of ionospheric anomalies to support use of GBAS in Category III weather conditions. This paper describes the results from modeling and simulation performed to explore the effectiveness of the ionospheric anomaly mitigations in the presence of multiple ionospheric plasma bubbles that regularly occur over the geomagnetic equator. The work also deals in general with the implications of multiple satellites being affected simultaneously by an ionospheric anomaly.

**Keywords:** GBAS, Category III, Ionospheric Anomaly, Standards.

## 1. INTRODUCTION

Disturbances in the ionosphere can result in non-differentially corrected errors in GBAS. Of particular concern are disturbances that create large spatial gradients in the delay experienced by GPS signals over a relatively short baseline (i.e. a few kilometers). This problem has been analyzed extensively in the course of implementing GBAS ground subsystems intended to support Category I (CAT I) operations, i.e. Facility Approach Service Type C (FAST C). A means to mitigate the effects of such ionospheric anomalies has been proposed [1] and incorporated in the latest revision of airborne standards [3][4][5][6][7][8]. The concept is also the basis for some requirements included in the revised airborne equipment MOPS [3] and ICD [8]. The proposal for mitigating the effects of the ionospheric anomalies relies on a combination of:

- Monitoring in the ground subsystem,
- Monitoring in the airborne segment,
- Siting restriction on the ground subsystem, and
- A standard threat space which defines the range of ionospheric anomalies to which the user will be exposed.

Working Paper 28 (Nov09/WP28) from the November 2009 ICAO Navigation Systems Panel (NSP) Category II/III Subgroup (CSG) meeting discusses a testing program that was done to evaluate the performance of these standard mitigations, which was summarized in

additional publications [1], [9]. The philosophy is to determine the largest errors that can persist after all the mitigation measures (i.e. monitors, baseline siting limitations and threat space limitations) have been applied. Appendix A of that paper gives a detailed discussion of the proposed mitigation elements and describes the simulation program used to evaluate the monitor performance in conjunction with siting constraints and threat space assumptions. Although that work was comprehensive in as far as it went, there were a number of unanswered questions that needed to be addressed.

Recent work described in this paper addresses the questions left unanswered by WP28 regarding the applicability of the wedge model effects as a bound on plasma bubble effects.

## 2. BACKGROUND

The proposed ionospheric anomaly mitigation scheme for GAST D has been described in detail in a number of previous papers [1][4]. Furthermore, specific requirements have been added to the airborne and ground requirements for GAST D [3][5]. The study described in [9] includes simulations of the performance of all the mitigations taken together. The study consists of an exhaustive computer simulation of the monitor performance across the full threat space proposed in [10] and for all possible combinations of geometry between the user, the runway and the ground station. Furthermore the

analysis considers all possible relative motions between the user and the ionospheric anomaly. The overall philosophy for requirements allocation between the ground, air and threat space for GAST D ionospheric anomalies was also presented in a companion paper developed for the November 2009 meeting [1].

The study in [9] shows the following:

- The study shows that the absolute largest error that can persist after all the mitigations have been applied is on the order of 2.75 meters in the pseudorange domain when considering a missed detection probability of  $1 \times 10^{-9}$ .
- The simulations show that different monitors are effective in different parts of the threat space. The monitors must be evaluated in concert with the siting limitations and for a defined threat space.
- The maximum errors appear to be insensitive to the exact nature of the speed profile of the approaching airplane. However, a speed change from typical cruising speeds to approach speeds is assumed.

The CSG discussed Nov09/WP 28 and agreed that there are a number of issues that required further work

- Real performance of the combination of these monitors hinges on feasibility of a very small threshold on the ground gradient monitor. More work is required to determine ground monitor feasibility and perhaps to better quantify RAIM FD performance.
- The study described in Nov 09/WP 28 had been done assessing the maximum error on a single pseudorange. It has been proposed that translation to position domain be accounted for by a simple assumption on projection into the position domain given geometry screening. This is a very conservative way to handle the effect of multiple satellite impacts. Furthermore, with plasma bubbles, the probability of multiple satellites being affected is non-trivial. Hence additional work is required to determine how the impact on multiple satellites can be addressed.
- Higher fidelity plasma bubble modeling is needed to assess the impact of ionospheric anomalies that affect multiple (e.g. 3+) satellites simultaneously.

Also at the November 2009 meeting, the CSG discussed NSP Nov 09 WGW/WP31 [1] which showed that some small disturbances in the ionosphere had been observed that appear to have a speed of propagation in excess of the limits currently proposed as a standardized threat model [10]. The group agreed that these fast moving anomalies should be considered and, if appropriate, the standard threat model should be modified accordingly.

Since the November 2009 meeting, the CSG ionospheric anomaly ad-hoc group has been engaged in addressing the outstanding questions described above. This paper discusses the work done and the conclusions that can be drawn from that work.

### 3. VALIDATION OF IONOSPHERIC ANOMALY MONITORING FOR GAST D

A high-fidelity modeling and simulation effort was undertaken to answer some of the issues requiring further work after the last meeting. Since a very simplified range domain model of the plasma bubble was used previously, and since that model maintained some wedge model specific assumptions, a three-dimensional ionosphere and plasma bubble model was coupled with a GPS constellation model to gather much higher fidelity results that could include the impact of more than two satellites impacted simultaneously by multiple plasma bubbles. This section describes the plasma bubble effect, the high-fidelity modeling of the bubble and its impact on the GAST D system, and results of the modeling and simulation.

#### 3.1 Overview of Plasma Bubble Effect

The plasma bubble is a local ionospheric plasma depletion that occurs in the low latitude region [1]. It accompanies sharp gradients in the ionospheric delay. The outstanding characteristics of the plasma bubble compared with the ionospheric front (or storm enhanced density: SED) observed over the United States are existence of a pair of gradients with opposite signs at the east and west edges of a plasma bubble and multiple plasma bubble appearance in series with several hundred kilometers separation as well as its very frequent occurrence in high solar activity. Therefore, it is often the case that there are multiple (two or more) gradients associated with plasma bubbles and multiple satellites can be impacted at the same time.

The general characteristics of a plasma bubble are illustrated in Figure 1. Since the plasma bubbles develop upward over the magnetic equator (and hence poleward in latitude), they are narrow in longitude, elongated in latitude, and the east and west edges are like steep walls, in general. It is expected that satellite-receiver paths along the walls of plasma bubbles at low elevation angles would be impacted the most, and those across the walls would be less. If this speculation was justified, then the impact of plasma bubbles on multiple satellites could be reduced (we would not have to give the maximum errors those satellites). For validating this, a two-dimensional ionospheric delay model is not sufficient, and a three-dimensional model is necessary.

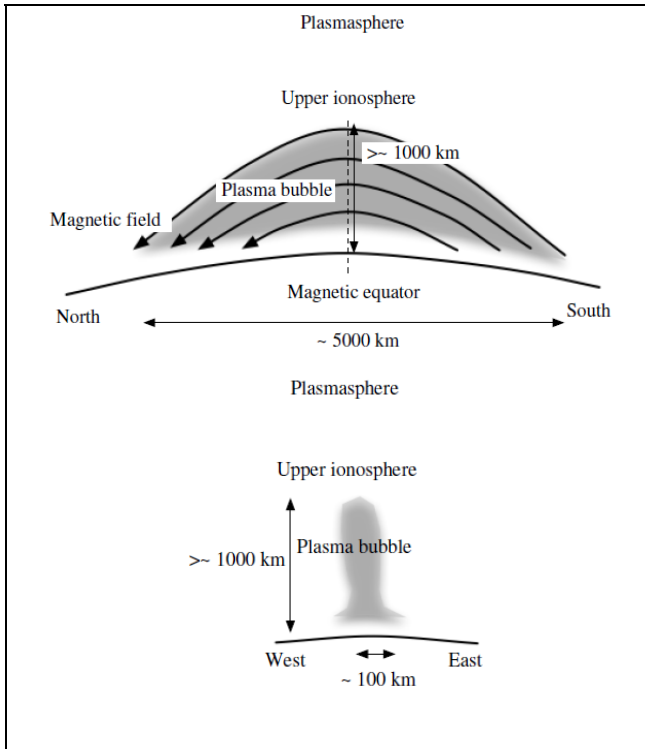


Figure 1 Equatorial Plasma Bubble Ionospheric Anomaly Visualization (North-South and East-West Perspectives)

According to the discussion above, the plasma bubble may impact multiple satellites, while impacts on some satellites may be potentially less significant. Therefore, we conducted exhaustive simulations with a three-dimensional ionospheric delay model to evaluate how many satellites can be impacted at the same time and how significant the impact is.

### 3.2 Three Dimensional Modeling of Plasma Bubbles

The three-dimensional ionosphere delay model consists of a background ionospheric model and a plasma bubble model. NeQuick was used as a background ionospheric model, which is an ionosphere model that is used to compute plasma density distribution between two arbitrary points, namely the GPS receiver and GPS satellites [12],[13],[14]. The earth's magnetic field is approximated by a dipole model. The background ionosphere is characterized by the following parameters:

- Geographic latitude, longitude, and altitude
- Date and time in UT
- Solar activity in terms of the solar radio flux index (F10.7) or the sunspot number index

Figure 2 shows an example global vertical Total Electron Count result from the NeQuick model that is used to represent the background ionosphere for this analysis [15]. Note that the largest TEC values happen at a particular time of day at the magnetic equator.

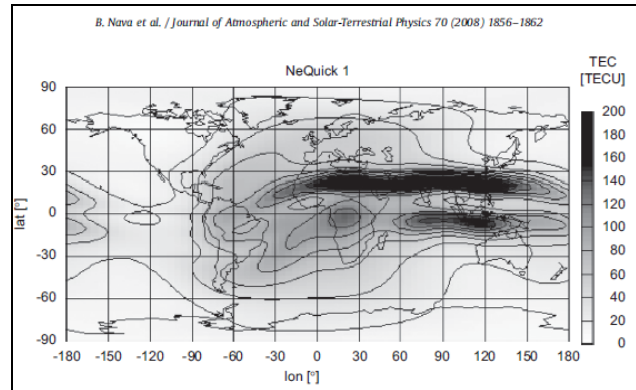


Figure 2 - Example Plot of Vertical TEC Based on NeQuick

This time and location is the general region that was chosen for the user location in these simulations.

A plasma bubble model is defined in the vertical plane in the magnetic equator given as relative depletion compared with background. By defining the plasma bubble shape in the magnetic equatorial plane and utilizing high magnetic conjugacy of the plasma bubble, the plasma bubble shape can be modeled in the 3-D space. So far, a very simple plasma bubble shape, a rectangle in the magnetic equatorial vertical plane, is used as illustrated in Figure 3. The plasma bubble moves zonally at a constant velocity. During the drift it is assumed to keep the same shape. A tilted-dipole magnetic field model is used to trace magnetic field line from an arbitrary point to the magnetic equatorial vertical plane. Parameters that have been implemented to characterize plasma bubbles are as follows:

- Number of plasma bubbles
- Positions at the magnetic equator
- Maximum depletion level relative to the background
- Height at the magnetic equator
- Zonal width
- Scale length of the plasma bubble boundary
- Zonal drift velocity

Ionospheric delays are calculated for a ground station fixed on the ground and an aircraft flying toward the ground station at a constant velocity. In our analysis, aircraft velocity of 80 meters per second is adopted. The output parameters from the model are as follows:

- Satellites' index in the field of view of the ground station
- Satellite position in the ECEF coordinate
- Non-carrier-smoothed delays for the ground station and the aircraft
- Difference between carrier-smoothed delays between the ground station and the aircraft.

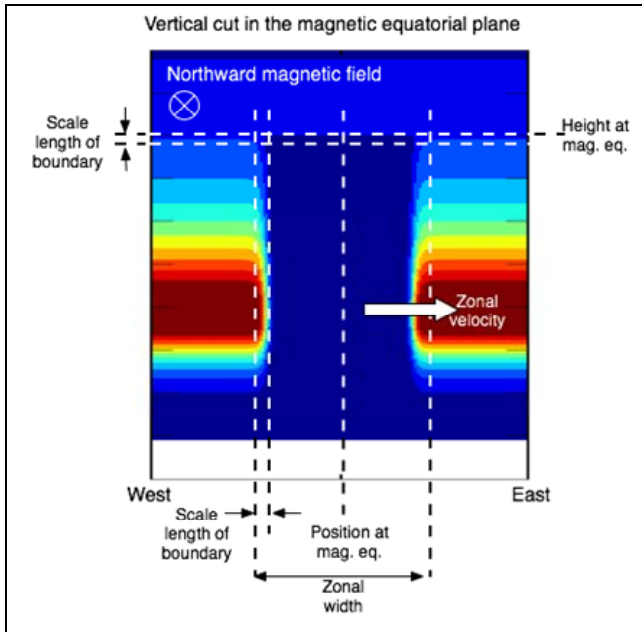


Figure 3 Simple Plasma Bubble Model

### 3.3 Ionospheric Anomaly Monitoring Algorithms

As described in the previous section, outputs of interest from the three-dimensional plasma bubble simulations are the airplane, reference, and satellite locations, and the non-carrier-smoothed ionosphere delay for each visible satellite at both the airplane and the reference locations.

The ionosphere code phase delay for each satellite and an opposite carrier phase advance are input into the carrier smoothing algorithm to produce a carrier-smoothed-code (CSC) error due to the ionosphere only. This is done for each satellite at the airplane and reference locations using both 100-second and 30-second smoothing time constants. Differential range error (DRE) due to the changing ionosphere is generated as the difference between the CSC errors at the airplane and reference receivers for both smoothing time constants.

The differential range error is saved for each satellite, and then the search for worst case scenarios begins. First the range domain ionosphere monitor outputs are determined, then a search is performed of all possible subset satellite geometries and their position domain geometry screens and ionosphere anomaly monitors. For the purposes of simulation, the ionosphere anomaly monitors are declared to detect after the ionosphere errors exceed the monitor threshold and an additional margin for measurement noise that is dependent on a desired missed detection probability for analysis. The ionosphere anomaly monitors are listed below; please see [9] for more detail on the implementation of these monitors in the simulation. The parameters  $S_{\text{vert}}$  and  $S_{\text{lat}}$  refer to the projections of range

measurements into the vertical and lateral components of the position solution.  $D_V$  and  $D_L$  refer to the difference between the 30-second and 100-second smoothed position solutions in the vertical and lateral.

Airborne and Reference Ionosphere Monitors:

- Airborne satellite geometry screening
  - $S_{\text{vert}}$ ,  $S_{\text{lat}}$ ,  $S_{\text{vert}2}$ ,  $S_{\text{lat}2}$ ,  $D_V$ ,  $D_L$ ,  $VPL_{\text{HO}}$ ,  $HPL_{\text{HO}}$
- Airborne RAIM fault detection
- Airborne code-carrier divergence monitor
- Reference code-carrier divergence monitor
- Reference absolute gradient monitor

### 3.4 Results of Plasma Bubbles Analysis

This section describes the range of parameters considered to develop simulation scenarios, assumptions made, and finally the simulation results from the scenarios.

#### 3.4.1 Scenarios and Assumptions

A range of scenarios were simulated to exhaustively search relative airplane, bubble, and satellite motion to find the worst case GAST D position errors. Figure 4 illustrates the model parameters that were varied during the study. A 100km wide, 1500km tall depletion region with 20km transition regions was used in a highly active ionosphere environment since this combination of the smallest observed plasma bubble dimensions among the largest background ionosphere delays was believed to have the potential to produce the largest differential position errors. Three plasma bubbles were included in the simulation with the second and third plasma bubbles at four degrees longitude East and West of the center bubble, and having the same dimensions and speed. The airplane speed was assumed to be a constant 80m/s. A constant airplane speed was expected to produce the worst case scenario since no benefit could be derived from the dual solution monitor during airplane speed changes. The airplane approach direction was varied in 90 degree increments, and three latitudes were chosen for the reference location: 0, 22, and 30 degrees magnetic latitude.

Simulation parameter search ranges:

- Approach direction (degrees heading)  
90, 180, 270, 360 (80m/s)
- Reference location (degrees latitude)  
0, 22, 35 (135 East Longitude)
- Plasma bubble speed (East meters per second)  
-100 : 10 : 200
- Plasma bubble phase ( $t = 0$  latitude, center bubble)  
132.6 : 0.1 : 136.9 ( $f(\text{speed})$ )
- Satellite constellation phase (simulation start time):  
24hrs at 10-minute intervals

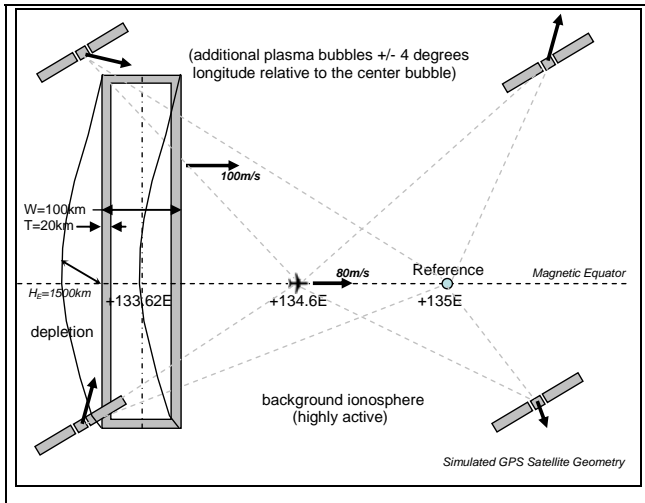


Figure 4 - Visualization of the Plasma Bubble Simulation Scenario

### 3.4.2 Simulation Results

Figure 5 through Figure 7 show example time histories of vertical ionospheric errors for each possible subset geometry for a single scenario. Figure 5 illustrates the vertical position errors that could result from the plasma bubbles for all possible geometries with four or more satellites out of the full set of satellites in view versus time and the VAL given that no geometry screening or ionospheric anomaly monitoring is performed. It is clear that the plasma bubble can impose a risk for some satellite geometries.

Next, Figure 6 illustrates the impact of simply screening out geometries using modest alert limits and projection limits, although this is merely an example, so the overall effectiveness of geometry screening will be shown later in this paper. Finally, Figure 7 shows that, for this example, airborne and reference CCD monitoring easily mitigates the effect of the plasma bubble. The maximum error that remains unmitigated at the threshold or touchdown at a distance, X, from the reference was chosen as a metric that could be collected for each scenario in an ‘exhaustive’ search of the trade space. The example chosen and shown in Figure 5 through Figure 7 leaves approximately two meters of vertical error unmitigated. Next, results for all of the scenarios are summarized.

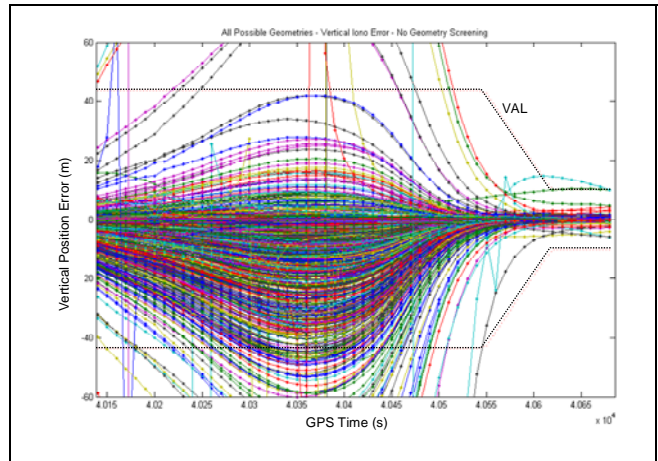


Figure 5 - Vertical Position Error versus Time for All Subset Geometries for an Example Plasma Bubble Scenario with No Geometry Screening and No Ionospheric Anomaly Monitoring Compared with Vertical Alert Limit

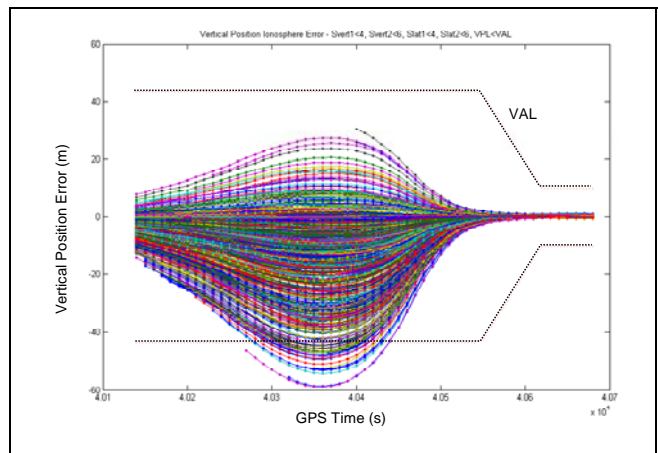


Figure 6 - Vertical Position Error versus Time for Only Those Subset Geometries Passing Geometry Screening Tests for the Example Plasma Bubble Scenario

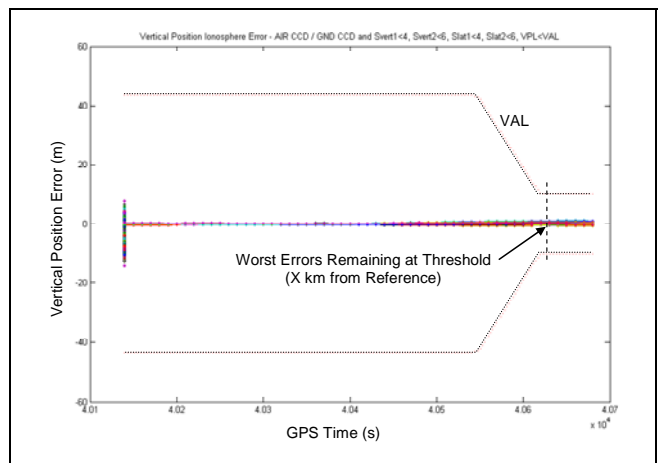


Figure 7 - Vertical Position Error versus Time for Only Those Subset Geometries Passing Geometry Screening Tests and Airborne and Reference CCD Monitors with  $10^{-9}$  Pmd for the Example Plasma Bubble Scenario

As described in the previous section, four approach directions were considered, along with multiple missed detection probabilities ( $P_{md}$ ) and geometry screening. Figure 8 summarizes the simulation results that have been collected to date for the 090 approach direction at a distance of 5.6 kilometers from the reference location. The results have been narrowed to those vertical position errors with  $P_{md} = 10^{-9}$  and for the worst case user location at each plasma bubble speed for three different assumptions about geometry screening. Three plots show the effect of increasingly strict limits on the total vertical projections of the two most influential satellites in the geometry (e.g.  $S_{vert2} < 6, 5, \text{ and } 4$ ).

The results in red represent the scenario with a reference location at 30 degrees North latitude. Errors up to 16 meters in these cases result from the fact that a very extreme background ionosphere was assumed. This results in up to 50 meters of slant range ionosphere delay that could transition to nearly zero ionosphere delay over a horizontal distance of 20 kilometers, which translates into a 2500 mm/km ionosphere gradient, which is well above the 500mm/km that was assumed feasible by the draft changes to the ICAO SARPs.

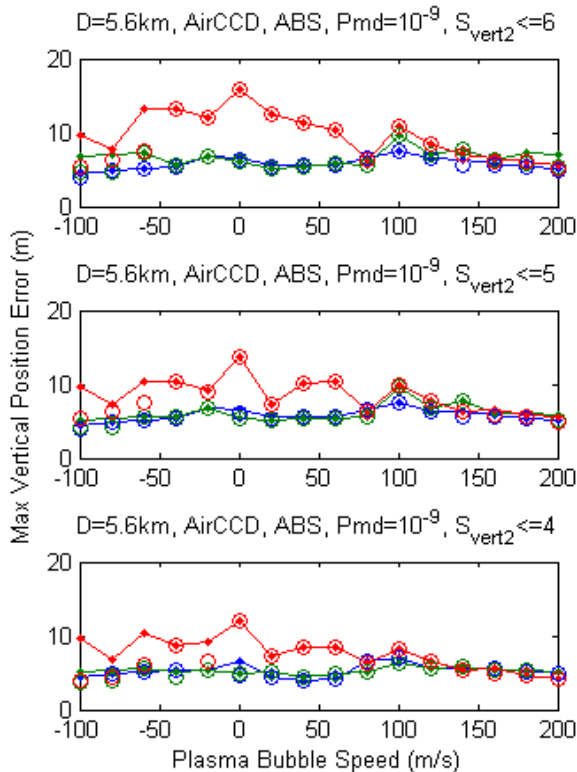


Figure 8 - Maximum Vertical Position Error at D=5.6km from Reference versus Reference Station Magnetic Latitude (0=blue, 22N=green, 30N=red), Plasma Bubble Ground Speed and Geometry Screening after Air CCD (dot) and Reference CCD Monitoring (circle), Dual Solution Monitoring, and Absolute Gradient Monitoring at the Reference Station

Figure 9 shows the same results as Figure 8 except that scenarios with gradients larger than 500 mm/km are not included. If larger gradients are considered feasible, then further work could be done by the service provider to determine if additional constraints on the GBAS installation are necessary, such as additional ionosphere monitoring, satellite geometry screening, or siting restrictions, for example.

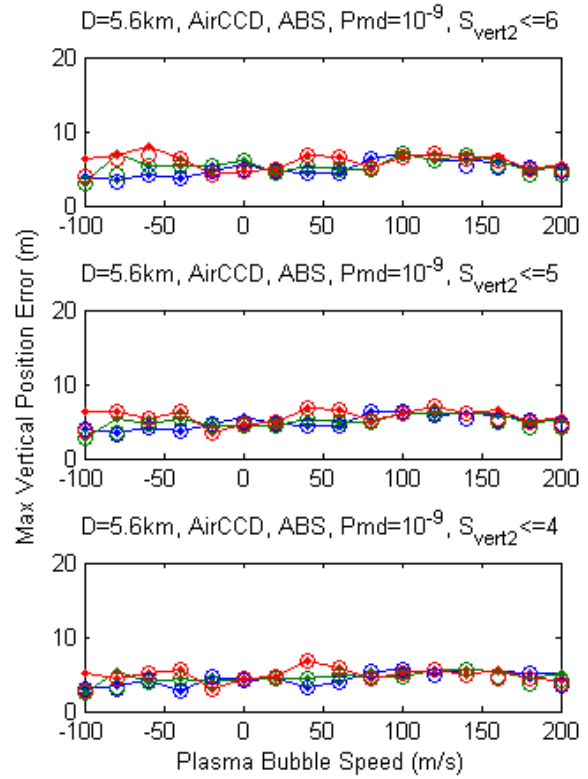


Figure 9 - Maximum Vertical Position Error at D=5.6km from Reference versus Reference Station Magnetic Latitude (0=blue, 22N=green, 30N=red), Plasma Bubble Ground Speed and Geometry Screening after Air CCD (dot) and Reference CCD Monitoring (circle), Dual Solution Monitoring, and Absolute Gradient Monitoring at the Reference Station, **All Cases With Max Gradient < 500mm/km**

#### 4. CONCLUSIONS

The analysis presented above, in conjunction with the range domain analysis based on the Ionospheric Wedge model presented in [9] supports the following conclusions:

1. The maximum vertical or horizontal position errors induced by an ionospheric anomaly that will persist (with a probability of greater than  $10^{-9}$ ) after all the ionospheric anomaly mitigations have been applied can be limited to less than 10 meters. Errors on the order of 10 meters or less have been shown to result in an airplane still landing in the safe landing box

- [1]. The maximum error can be reduced somewhat by using more aggressive geometry screening.
2. The ground gradient monitor plays an important role in limiting the error magnitudes when anomaly speeds are near the aircraft pierce point speeds.
3. A 5 km baseline siting restriction appears to provide adequate performance. Although some possibility to relax this restraint still exists, it is recommended that 5 km be adopted as the baseline and that future work be undertaken during the operational validation phase to determine if this siting restriction can be relaxed or if additional siting flexibility can be achieved in some other way.
4. The general rule that the maximum error in the pseudorange domain of 2.75 meters (postulated in [9]) appears to hold for plasma bubbles as well as the wedge model. This maximum error characterization can be used in the formulation of a fault model for use in airworthiness assessments.
5. The conservative approach of accounting for multiple satellite by geometry limiting based on  $S_{\text{vert}2}$  or  $S_{\text{lat}2}$  appears valid since no more severe effects have been found using the high fidelity 3-D plasma bubble in conjunction with a satellite geometry simulation than were found with the pseudorange domain wedge model as scaled by  $S_{\text{vert}2}$  limits.

As mentioned above, as a part of the operational validation phase, the full complement of planned simulations will be completed to verify that no unexpected large errors result from scenarios not yet modeled.

## 5. ACKNOWLEDGMENTS

The authors would like to thank the ICAO Navigation Systems Panel Category II/III Sub Group for their review and inputs regarding this work, particularly all of those who participated in the ionospheric anomaly ad-hoc group.

## 6. REFERENCES

- [1] ICAO NSP/WG1 WP 26, "Mitigation of Iono Gradient Threat for GSL D", New Delhi, March 6<sup>th</sup> 2007
- [2] Harris, Matt; Murphy, Tim; "Putting the Standardized GBAS Ionospheric Anomaly Monitors to the Test", Proceedings of the ION GPS 2009, Dallas, TX, USA, Sept 2009.
- [3] RTCA DO-253C "Minimum Operational Performance Standards for GPS Local Area Augmentation System Airborne Equipment", Dated Dec 16 2008.
- [4] ICAO NSP WG1/WP29 " Ionospheric Anomaly Detection Requirements for GAST D" March 09.
- [5] ICAO NSP/CSG, "Flimsy 9: GAST D GBAS SARPS Draft - Baseline Post Seattle Meeting," presented by Tim Murphy, Seattle, WA, July 2009.
- [6] NSP/CSG/Toulouse, July 2008, WP-12 "Proposed SARPS Changes for GAST-D".
- [7] NSP/WGW/Montreal, Oct 2008, WP-XX "Proposed SARPS Changes for GAST-D".
- [8] RTCA DO-246C – "GNSS Based Precision Approach Local Area Augmentation System (LAAS) - Signal-in-Space Interface Control Document (ICD)".
- [9] ICAO NSP WG1/WP 28, " Validation of GAST D Mitigation of Errors Induced by Ionospheric Decorrelation ", Montreal, November 2009.
- [10] ICAO NSP WG1/WP 29, " Standard Threat Model Used in GAST D Ionospheric Monitoring Validation ", Montreal, November 2009.
- [11] ICAO NSP Nov 09 WG1/WP31, " GBAS Ionosphere Threat Model Validation in Germany", Montreal, November 2009.
- [12] S. Saito, T. Yoshihara, and N. Fujii, "Study of Effects of the Plasma Bubbles on GBAS by a Three-Dimensional Ionospheric Delay Model," Proceedings of ION GNSS 2009, Savannah, GA, USA, Sept. 22-25, 2009.
- [13] G. di Giovanni, G. and S. R. Radicella, "An analytical model of the electron density profile in the ionosphere", Adv. Space Res., 10, 27-30, 1990.
- [14] S. M. Radicella, and M. L. Zhang, "The improved DGR analytical model of electron density height profile and total electron content in the ionosphere", Annali di Geofisica, 38, 35-41, 1995.
- [15] Nava, B., et. al., "A new version of the NeQuick ionosphere electron density model", Journal of Atmospheric and Solar-Terrestrial Physics, 70, 1856-1862, 2008.
- [16] Murphy, T.; Anderson, L.; Harris, Matt; Tang, N. "CAT III Simulated Landing Performance for ILS and GLS", Proceedings of the ION GPS 2001, Sept 2001, Salt Lake City.

## 7. COPYRIGHT

The authors confirm that they, and/or their company or institution, hold copyright of all original material included in their paper. They also confirm they have obtained permission, from the copyright holder of any third party material included in their paper, to publish it as part of their paper. The authors grant full permission for the publication and distribution of their paper as part of the EIAC2008 proceedings or as individual off-prints from the proceedings.